Chemistry Europe
European Chemical Societies Publishing

WILEY VCH

Excellence in Chemistry Research

Announcing our new flagship journal

- Gold Open Access
- Publishing charges waived
- Preprints welcome
- Edited by active scientists

Meet the Editors of *ChemistryEurope*

Luisa De Cola
Università degli Studi di Milano Statale, Italy

Ive Hermans
University of Wisconsin-Madison, USA

Ken Tanaka
Tokyo Institute of Technology, Japan

Chemistry–A European Journal
Research Article
doi.org/10.1002/chem.202301945
Chemistry Europe
European Chemical Societies Publishing
www.chemeurj.org

Hot Paper

(Bio)Functionalisation of Metal–Organic Polyhedra by Using Click Chemistry

Laura Hernández-López,[a, b] Cornelia von Baeckmann,[a, b] Jordi Martínez-Esaín,[a] Alba Cortés-Martínez,[a, b] Jordi Faraudo,[c] Caterina Caules,[a, b] Teodor Parella,[d] Daniel Maspoch,*[a, b, e] and Arnau Carné-Sánchez*[a, b]

The surface chemistry of Metal–Organic Polyhedra (MOPs) is crucial to their physicochemical properties because it governs how they interact with external substances such as solvents, synthetic organic molecules, metal ions, and even biomolecules. Consequently, the advancement of synthetic methods that facilitate the incorporation of diverse functional groups onto MOP surfaces will significantly broaden the range of properties and potential applications for MOPs. This study describes the use of copper(I)-catalysed, azide–alkyne cycloaddition (CuAAC) click reactions to post-synthetically modify the surface of alkyne-functionalised cuboctahedral MOPs. To this end, a novel Rh(II)-based MOP with 24 available surface alkyne groups was synthesised. Each of the 24 alkyne groups on the surface of the "clickable" Rh-MOP can react with azide-containing molecules at room temperature, without compromising the integrity of the MOP. The wide substrate catalogue and orthogonal nature of CuAAC click chemistry was exploited to densely functionalise MOPs with diverse functional groups, including polymers, carboxylic and phosphonic acids, and even biotin moieties, which retained their recognition capabilities once anchored onto the surface of the MOP.

Introduction

As a subclass of molecular cages assembled from metal-ions and organic linkers, Metal–Organic Polyhedra (MOPs) exhibit unique porosity capabilities: for example, they can host molecules in solution and are permanently porous in the solid state. Importantly, most of these materials fall within the nanoscale regime, having outer diameters of ~2 nm to 5 nm. This is especially true for the archetypical cuboctahedral $[M_2(m\text{-bdc})_2]_{12}$ MOP (where *m*-bdc is isophthalate), which resembles a spherical ~2.5 nm-in-diameter molecular nanoparticle.[1] As such, as in inorganic nanoparticles, most of its physicochemical properties (e.g. solubility, recognition, and assembly) rely on its surface chemistry.[2–11] For instance, on its outer surface this cuboctahedral MOP contains up to 84 potential sites that can be used to introduce new functionalities: 72 that stem from positions 4, 5, and 6 of the aromatic organic linkers, and 12 that belong to the axial metal sites.

Among the existing functionalisation strategies, copper(I)-catalysed azide–alkyne cycloaddition (CuAAC), commonly known as click chemistry, is probably the most popular, powerful, and versatile chemical tool to post-synthetically modify molecules and materials.[12–14] This is mainly due to its quantitative and orthogonal reactivity, which makes it compatible with myriad functional groups and even biomolecules.[15,16] However, the straightforward use of CuAAC for the post-synthetic modification of MOPs presents several challenges due to the instability of coordination bonds to common click chemistry reagents (e.g., reducing agents and metal salts).[17] Therefore, researchers have developed alternative reaction conditions for the CuAAC reaction to avoid the use of reducing agents. These conditions involve the use of Cu(I) complexes as catalysts,[6] or of the strain-promoted version of the azide–alkyne cycloaddition, the latter of which has been employed for most partial modifications of parent cages.[18,19] Only very recently did Bloch and co-workers show that robust rectangular prismatic MOPs assembled from Co(II) calixarene-capped clusters and 5-azido isophthalic acid (5-N_3-bdc) or 5-propargyl isophthalic acid can withstand the reaction conditions of the classical CuAAC reaction.[20] Indeed, they reported the quantita-

[a] L. Hernández-López, Dr. C. von Baeckmann, Dr. J. Martínez-Esaín, A. Cortés-Martínez, C. Caules, Prof. Dr. D. Maspoch, Dr. A. Carné-Sánchez
Catalan Institute of Nanoscience and Nanotechnology (ICN2)
CSIC and The Barcelona Institute of Science and Technology
Campus UAB, Bellaterra, 08193 Barcelona (Spain)
E-mail: arnau.carne@icn2.cat
daniel.maspoch@icn2.cat
[b] L. Hernández-López, Dr. C. von Baeckmann, A. Cortés-Martínez, C. Caules, Prof. Dr. D. Maspoch, Dr. A. Carné-Sánchez
Departament de Química, Facultat de Ciencies
Universitat Autonoma de Barcelona, 08193 Bellaterra (Spain)
[c] Dr. J. Faraudo
Institut de Ciència de Materials de Barcelona (ICMAB-CSIC)
08193 Bellaterra (Spain)
[d] Dr. T. Parella
Servei de Ressonància Magnètica Nuclear
Universitat Autònoma de Barcelona
Campus UAB, Bellaterra, 08193 Barcelona (Spain)
[e] Prof. Dr. D. Maspoch
ICREA
Pg. Lluís Companys 23, 08010 Barcelona (Spain)

Supporting information for this article is available on the WWW under https://doi.org/10.1002/chem.202301945

tive conversion of 4 pendant alkyne or azide groups of the MOP through this reaction run at high temperature.

Herein we have adapted and optimised CuAAC to enable covalent functionalisation of up to 24 positions of cuboctahedral Rh-MOPs[21] with a diverse repertoire of molecules. To this end, we initially introduced an alkynyl group onto position 5 of the aromatic organic linker of a 24-functionalized cuboctahedral Rh-MOP through a protection/deprotection method,[22] forming a "clickable" Rh-MOP with formula [Rh_{24}(ethynyl-bdc)$_{24}$] (hereafter named BCN-23; where ethynyl-bdc is 5-ethynyl-1,3-benzenedicarboxylate). Afterwards, we demonstrated that each of the 24 alkyne groups located on the outer surface of the cuboctahedron could be reacted at room temperature with azide-containing molecules without compromising the integrity of the MOP. Thus, we used click chemistry to quantitively and densely functionalise the surface of BCN-23 with a wide range of functionalities that could not otherwise be easily introduced (e.g. by direct synthesis or current post-synthetic approaches). These functionalities include polymers, free carboxylic acid groups, free phosphonic acid groups, and bioactive biotin molecules. Furthermore, we proved that addition of these functionalities modulates the properties (e.g. solubility) of BCN-23, and that the biorecognition capabilities of biotin moieties grafted onto the surface of BCN-23 to avidin are preserved.

Results and Discussion

Synthesis of the "clickable" alkyne-terminated Rh-MOP

Traditionally, cuboctahedral Rh-MOPs are synthesised through a solvothermal reaction between Rh_2Ac_4 and the corresponding linker. However, BCN-23 cannot be synthesised this way because the linker ethynyl-bdc is not stable at high temperatures or under basic conditions. Thus, we developed a protection-deprotection strategy that entailed the synthesis of the alkyne-protected Rh-MOP and its subsequent deprotection to finally yield the targeted clickable MOP (Figure 1). Triisopropylsilyl was selected as a protecting group because of its compatibility with the linker and the synthetic conditions required to make Rh-MOPs, including the use of high temperatures and basic conditions. Thus, after reacting dimethyl 5-iodoisophtalate with (triisopropylsilyl)acetylene and subsequently deprotecting the carboxylic groups, the protected version of ethynyl-bdc, 5-((triisopropylsilyl)ethynyl))isophthalic acid (TIPS-bdc), was obtained. Next, TIPS-bdc was reacted with Rh_2Ac_4 in DMA at 100 °C in the presence of Na_2CO_3 for 48 h to yield a MOP with formula [Rh_{24}(TIPS-bdc)$_{24}$] (yield: 80 %) (Figure 1a). The formation of the alkyne-protected Rh-MOP was confirmed by matrix-assisted laser desorption/ionisation-time-of-flight (MALDI-TOF) spectroscopy, which showed a signal at 11024.5 m/z, which closely agrees with the targeted cuboctahedral Rh(II)-MOP ([Rh_{24}(TIPS-bdc)$_{24}$ + H^+]$^+$ · 2DMA · 2MeOH, expected m/z = 11024.9) (Figure S4). The ^{1}H NMR spectrum of the alkyne-protected MOP in $CDCl_3$-d_1 further confirmed the synthesis of a discrete metal–organic assembly with 24 triisopropylsilyl protecting groups on its surface (δ = 1.05 ppm; Figure S1). Furthermore, diffusion-ordered spectroscopy (DOSY) NMR analysis showed the same diffusion coefficient of $3.7 \cdot 10^{-10}$ $m^2 s^{-1}$ for the aromatic and protecting group protons, which further corroborated that both moieties belong to the same metal–organic structure (Figure S2). The integrity of the Rh–Rh paddlewheel was confirmed through UV-Vis spectroscopy in chloroform, which showed the characteristic band centred at 630 nm, which corresponds to Band I of the Rh–Rh paddlewheel (Figure S4).

The alkyne-available Rh-MOP (BCN-23) was synthesised by treating a THF solution of the alkyne-protected MOP with 36 mol. equiv. of tetrabutylammonium fluoride (TBAF) solution (1.0 M in THF) (Figure 1b). Upon addition of the TBAF solution, a blue precipitate was immediately formed. This solid was collected by centrifugation, washed with THF and finally, dissolved in DMSO for further analysis (yield: > 95 %). The ^{1}H NMR spectrum of BCN-23 in DMSO-d_6 confirmed the quantitative fading of the peaks ascribed to the TIPS protecting group, together with the appearance of a new signal at 4.3 ppm (Figure S5), which corresponds to the alkyne proton. The aromatic and alkyne protons showed the same diffusion coefficient of $6.5 \cdot 10^{-11}$ $m^2 s^{-1}$ in the DOSY ^{1}H NMR data (Figure S6). The hydrodynamic radius of BCN-23 was calculated to

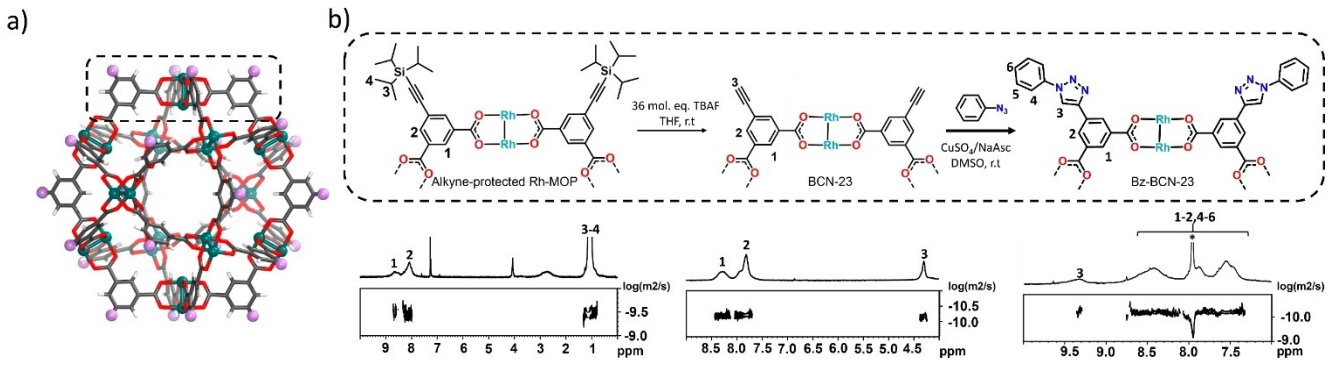

Figure 1. (a) Schematic of the cuboctahedral Rh-MOP, highlighting the positions at which the CuAAC click reaction is performed. (b) Schematic showing the synthesis of the "clickable" BCN-23 MOP, and its subsequent post-synthetic modification with azidobenzene through a CuAAC (top), with the corresponding ^{1}H-NMR spectra and DOSY NMR representation for each synthetic step (bottom). NMR data for the alkyne-protected Rh-MOP was obtained in $CDCl_3$-d_1 whereas the DMSO-d_6 was used for BCN-23 and Bz-BCN-23.

be approximately 1.7 nm, which agrees with the value obtained from the computer simulation of this structure (Figure S7).[18] MALDI-TOF analysis of BCN-23 was characterised by a single broad peak centred at 7061.6 m/z, which closely agrees with the expected mass of 7064.1 m/z for the targeted formula $[Rh_{24}(ethynyl\text{-}bdc)_{24}+H^+]^+\cdot DMSO$ (Figure S9). Additionally, the integrity of the Rh–Rh paddlewheel after the deprotection reaction was further confirmed by UV-Vis spectroscopy in DMF, which showed the characteristic band centred at 589 nm that corresponds to Band I of the Rh–Rh paddlewheel (Figure S9). Altogether, these results corroborate the successful synthesis of BCN-23 as a cuboctahedral Rh-MOP functionalised with 24 available alkyne groups on its outer surface.

CuAAC click reactions on BCN-23: functionalisation with small and polymeric azide molecules as model substrates

We initially assessed the reactivity and functionalisation of BCN-23 through CuAAC click chemistry using azidobenzene as our model azide compound. To this end, 36 mol. equiv. of azidobenzene per MOP unit (i.e. 1.5 mol. equiv. of azidobenzene per alkyne group) were added to a DMSO solution of BCN-23 followed by the stepwise addition of $CuSO_4$ (1.5 mol. equiv. per alkynyl group) and sodium ascorbate (4.5 mol. equiv. per alkynyl group, 3 mol. equiv. per Cu(II)). The reaction mixture was left to react overnight at room temperature. The reaction proceeded under homogenous conditions: no precipitate was observed throughout the reaction. The product of the reaction (hereafter named Bz-BCN-23) was precipitated out by adding ethyl acetate as counter solvent, and further purified through successive washing with 1:2 mixtures of DMF/HCl (0.3 M) and of DMF/water (yield: 95%).

The UV-Vis spectrum of Bz-BCN-23 in DMF showed a $\lambda_{max}=$ 590 nm, which confirmed the integrity of the Rh(II) paddlewheel unit through the catalytic reaction (Figure S19). This result corroborated that Rh(II) is not reduced upon addition of ascorbic acid or exchanged in the presence of Cu(II). Furthermore, UV-Vis spectrum of Bz-BCN-23 also confirmed that the newly formed triazole ring does not coordinate to the exposed Rh(II) axial sites due to the strong steric hindrance around the coordinating N atoms of the triazole ring.[24] MALDI-TOF analysis revealed a single broad peak centred at 10045 m/z, which closely agrees with the expected molecular mass for $[Rh_{24}(5\text{-}(1\text{-}phenyl\text{-}1H\text{-}1,2,3\text{-}triazol\text{-}4\text{-}yl)\text{-}bdc)_{24}+H^+]^+\cdot DMF\cdot 3H_2O$ (expected = 10045 g/mol) (Figure S19). ^{1}H NMR analysis of a DMSO-d_6 solution of Bz-BCN-23 showed a downfield shift of the aromatic protons of the BDC moiety, and the appearance of a new broad aromatic signal at $\delta=7.55$ ppm, which corresponds to the incorporated phenyl moiety on the surface of the MOP (Figure S11). Furthermore, the formation of the triazole ring linking the MOP unit to the phenyl ring was first evidenced by the appearance of a signal at $\delta=9.35$ ppm, which corresponds to the olefinic proton of the triazole ring, and by the quantitative fading of the signals of the alkyne protons groups ($\delta=4.30$ ppm, Figure S10). Supporting this later observation, the Fourier transform infrared spectroscopy (FTIR) spectrum of Bz-BCN-23 revealed complete disappearance of the stretching band corresponding to the alkyne group at 3284 cm^{-1} (Figure S20). DOSY NMR data of Bz-BCN-23 showed the same diffusion coefficient ($5.3\cdot10^{-11}$ m^2 s^{-1}) for all aromatic protons (Figure 1b and S12). The calculated hydrodynamic radius was found to be 2.1 nm, in agreement with the equilibrium configuration of the simulated structure (Figure S21).

Further evidence of the quantitative conversion of the alkyne groups was provided by the ^{1}H NMR analysis of the acid-digested Bz-BCN-23. The spectrum of the digested Bz-BCN-23 showed only the signals corresponding to 5-(1-phenyl-1H-1,2,3-triazol-4-yl)-bdc, which is the linker expected to be created upon coupling of the initial 5-ethynyl-bdc linker of BCN-23 to azidobenzene via CuAAC (Figure S13). Finally, as expected for this type of click reaction, only the 1,4-substituted triazole ring was formed, as confirmed by the ROESY NMR data of the digested Bz-BCN-23 (Figure S18).

From the above model reaction, we corroborated that all 24 alkyne groups on the outer surface of BCN-23 can be reacted through CuAAC click chemistry with an azide group without compromising the integrity of the Rh-MOP. To further confirm this quantitative functionalisation, we next targeted the functionalisation of BCN-23 with a polymer, to form a polymer grafted Rh-MOP.[6,7,25,26] To this end, BCN-23 was reacted with 36 mol. equiv. (i.e. 1.5 mol. equiv. per alkynyl group) of an azide terminated polyethylene glycol polymer ($mPEG_{42}$-N_3) with 42 repeating units (average molecular weight $=2000\pm300$ g/mol) overnight at room temperature. As for the previous click reaction, this reaction also proceeded homogenously in DMSO. The resulting PEGylated Rh-MOP (hereafter named $mPEG_{42}$-BCN-23) was isolated by precipitation from the reaction mixture with diethyl ether, collected by centrifugation, and then purified (yield: >95%).

The ^{1}H NMR spectrum of the PEGylated Rh-MOP in MeOD-d_4 showed a broad signal in the aromatic region at *ca.* $\delta=$ 8.54 ppm, which corresponds to the bdc and to the triazole moieties (Figure S22). Additionally, it showed peaks at $\delta=$ 3.64 ppm, corresponding to the aliphatic ethylene glycol units. Both sets of signals belong to the same molecule, as confirmed by DOSY experiments on $mPEG_{42}$-BCN-23 that revealed a diffusion coefficient of $8.1\cdot10^{-11}$ m^2 s^{-1} (Figure S23). The calculated hydrodynamic size of $mPEG_{42}$-BCN-23 was 4.9 nm. These results reflected a considerable increase in the hydrodynamic radius relative to the previously found values, supporting the notion that the PEG chains were indeed attached to the surface of BCN-23.

Next, to elucidate the degree of PEGylation, we analysed the digested $mPEG_{42}$-BCN-23 by ^{1}H NMR. The spectrum of the digested $mPEG_{42}$-BCN-23 in DMSO-d_6 revealed that all 24 5-ethynyl-bdc linkers of the parent BCN-23 had been clicked with the polymer chains (Figure S24). The quantitative PEGylation of BCN-23 was further confirmed by MALDI-TOF analysis of $mPEG_{42}$-BCN-23, which showed a broad peak at *ca.* 53470.5 g/mol, which corresponds to a PEGylated Rh-MOP with formula $([Rh_{24}(5\text{-}(mPEG_{42}\text{-}1H\text{-}1,2,3\text{-}triazol\text{-}4\text{-}yl)\text{-}bdc)_{24}+H^+]^+\cdot 20MeOH$ (expected m/z = 53468.4) (Figure 2 and Figure S28). Also, FTIR analysis of $mPEG_{42}$-BCN-23 revealed the complete disappear-

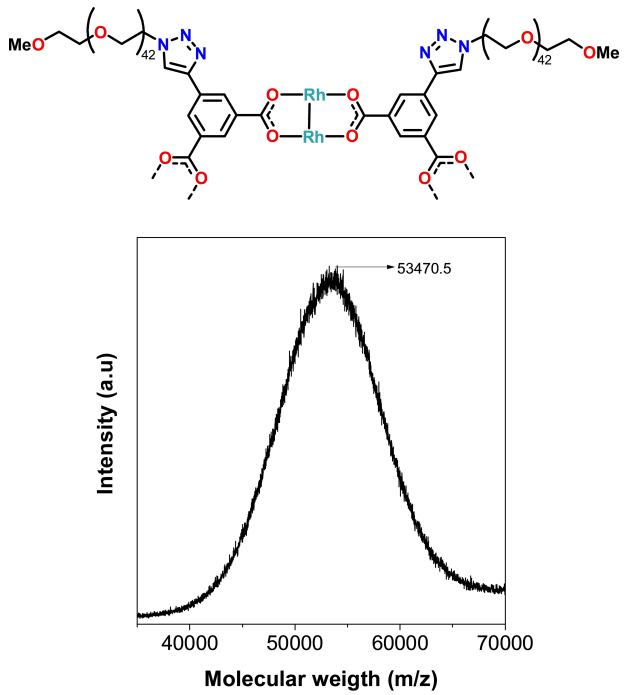

Figure 2. Schematic showing the structure of $mPEG_{42}$-BCN-23 (top) and the corresponding MALDI-TOF spectrum (bottom). The molecular weight corresponding to the formula ($[Rh_{24}$(5-($mPEG_{42}$-*1H*-1,2,3-triazol-4-yl)-bdc)$_{24}$ $+H^+]^+ \cdot 20MeOH$ has been highlighted: expected m/z = 53468.4; found m/z = 53470.5.

ance of the stretching band at 3284 cm^{-1}, further confirming that all the alkyne groups on the surface of the MOP had been reacted (Figure S29). Importantly, due to the quantitative PEGylation, the physicochemical properties of the product were drastically different from those of the initial BCN-23. For example, whereas the initial BCN-23 is only soluble in DMSO and DMF, the densely PEGylated $mPEG_{42}$-BCN-23 exhibits a broad solubility profile, covering most organic solvents such as methanol, chloroform, DMF and DMSO and water in a wide range of pH values (Figure S27).

Functionalisation of BCN-23 with carboxylic and phosphonic acid groups

Having demonstrated the regioselective and quantitative nature of click chemistry on the alkyne surface groups of BCN-23, we next sought to take advantage of the orthogonal reactivity of this chemistry to decorate the surface of BCN-23 with coordinating groups such as carboxylic or phosphonic acid groups. The formation of MOPs with surface-available carboxylic or phosphonic acid groups is very challenging, as these groups tend to react with metal ions, thus precluding formation of the desired MOP. Indeed, there is only one reported example of a covalent COOH-functionalised MOP, which was prepared through a post-synthetic protection/deprotection strategy, and there are no reports of any phosphonic acid-functionalised MOPs.[22] To prove that the CuAAC reaction could be used to post-synthetically functionalise MOPs with available carboxylic or phosphonic acid groups, we ran experiments with four azide substrates: three terminated with carboxylic acid groups (azidobenzoic acid, 6-azidohexanoic acid, and COOH-PEG_3-N_3) and one terminated with a phosphonic acid group (H_2PO_3-PEG_3-N_3). The reaction of BCN-23 with azidobenzoic acid (36 mol. equiv.), 6-azidohexanoic acid (36 mol. equiv.) or COOH-PEG_3-N_3 (36 mol. equiv.) in the presence of $CuSO_4$ (1.5 mol. equiv.), sodium ascorbate (2.25 mol. equiv.) and HCl (0.0031 mol. equiv.) in DMSO yielded three new COOH-functionalised MOPs: COOH–Bz-BCN-23 (yield: >95%), COOH–C_5-BCN-23 (yield: >95%), and COOH-PEG_3-BCN-23 (yield: >95%) (Figure 3). It is important to note here that the addition of HCl to the catalytic reaction was required to prevent coordination of the free carboxylic acid groups to the copper catalyst. In all cases, the click reaction was quantitative, as evidenced by the ^1H NMR spectra of the corresponding acid-digested samples (Figur-

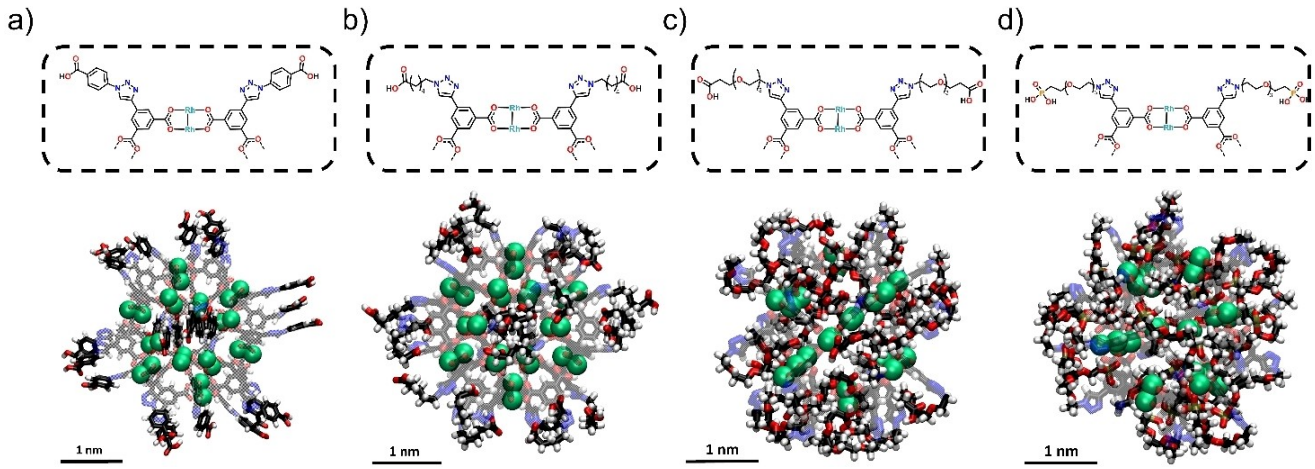

Figure 3. Schematic composition (top) and simulated structure (bottom) of COOH–Bz-BCN-23 (a), COOH-C_5-BCN-23 (b), COOH-PEG_3-BCN-23 (c) and H_2PO_3-PEG_3-BCN-23 (d). The structure shown corresponds to snapshots of the equilibrium configuration obtained in the computer simulations (snapshots made with VMD).[23] Color code: Rhodium (green); carbon (black); hydrogen (white); oxygen (red); nitrogen (blue); phosphor (gold). Rh atoms are shown in their Van der Waals size while linker is represented with Licorice drawing method. For simplicity, the MOP core is displayed as translucent.

es S32, S39, and S46, respectively). Moreover, DOSY NMR analysis of the three COOH-functionalised MOPs in DMSO-d_6 corroborated the successful coupling of the COOH moiety onto the surface of the BCN-23 unit (Figures S31, S38, and S45 respectively). The estimated hydrodynamic radii values derived from the DOSY NMR representation were found to be 2.2 nm (COOH–Bz-BCN-23), 1.9 nm (COOH-C_5-BCN-23), and 2.5 nm (COOH-PEG_3-BCN-23). These values are in agreement with the simulated structures (Figure 3a, 3b and 3c). Furthermore, the simulations also revealed the orientation of the three types of carboxylic acids on the surface of the MOP core. Whereas the carboxylic acids of COOH–Bz-BCN-23 and COOH–C5-BCN-23 are stretched out from the MOP core, the PEG chains of the COOH-PEG_3-BCN-23 are wrapped around the MOP core, in what is called "mushroom" configuration in nanoparticles.[27]

MALDI-TOF analysis also proved that, upon reaction of BCN-23 with each of the three types of carboxylic acid substrates separately, each functionalised product has a higher molecular weight than the starting MOP. In all cases, a broad signal containing the expected molecular formula for each acid derivative of BCN-23 was observed (Figures S33, S40, and S47, respectively). Free carboxylic acid groups were also evident in the FTIR spectrum of all three COOH-functionalised MOPs, which showed a new stretching C=O band centred at *ca.* 1728 cm^{-1} that corresponds to the presence of free carboxylic acid groups (Figures S35, S42, and S49). Therefore, CuAACs enable not only the synthesis of COOH-functionalised MOPs but also enable control over the type (i.e. aliphatic or aromatic) and length of the spacer between the MOP core and the surface carboxylic acid groups.

Next, we challenged our approach by attempting the synthesis of the first ever MOP functionalised with available phosphonic acid groups. Free phosphonic acids are highly coordinating groups that are generally incompatible with metal–organic structures, although they have been used to build up extended structures as an alternative to the metal-carboxylate bond.[28,29] However, we found BCN-23 to be stable against free phosphonic acids such as phenylphosphonic acid, which encouraged us to pursue its post-synthetic functionalisation with pendant phosphonic acid groups (Figure S56). The click reaction between BCN-23 and H_2PO_3-PEG_3-N_3 (36 mol. equiv.) was performed in the presence of the previously employed catalytic mixture comprising $CuSO_4$ (0.25 mol. equiv. per alkynyl group) and sodium ascorbate (7.5 mol. equiv. per alkynyl group, 30 mol. equiv. per Cu(II) ion). Moreover, in this case, we also added the chelating agent tris-hydroxypropyltriazolylmethylamine (THPTA) to the mixture to prevent coordination of the phosphonate groups to the copper catalyst. After 1 h of reaction at room temperature, a precipitate (hereafter named H_2PO_3-PEG_3-BCN-23) was obtained, isolated by centrifugation, and subsequently washed with 0.3 M HCl and water (yield: 87%). The integrity of the Rh(II) paddlewheel in H_2PO_3-PEG_3-BCN-23 was first confirmed by the presence of the characteristic $\lambda_{max} = 582$ nm in the UV-Vis spectrum (Figure S54). Furthermore, the ^{1}H NMR spectrum of H_2PO_3-PEG_3-BCN-23 in D_2O revealed the disappearance of the alkyne protons and the appearance of broad PEG and aromatic signals, which had the same diffusion coefficient of $7.2 \cdot 10^{-11}$ m^2 s^{-1}, as determined by DOSY NMR (Figures S51 and S52, respectively). The calculated hydrodynamic radius was 2.6 nm, in agreement with the simulated structure. As in the case of COOH-PEG_3-BCN-23 the PEG chains are wrapped around the MOP core (Figure 3d).

The MALDI-TOF spectrum of COOH-PEG_3-BCN-23 revealed a broad peak with a centred m/z value of 13855.5 g/mol, in good agreement with a Rh-MOP of formula [Rh_{24}(5-phosphono-PEG_3-(−1H-1,2,3-triazol-4-yl)-bdc)$_{24}$ + H^+]$^+$ · $4H_2O$ (expected m/z for this formula = 13855.0) (Figure S54). The presence of the free phosphonic acid group on H_2PO_3-PEG_3-BCN-23 was further confirmed by FTIR, which exhibited the characteristic band centred at 1044–1046 cm^{-1} (Figure S57). Altogether, these results demonstrate that BCN-23 is stable under homogenous conditions in the presence of free phosphonic acids and chelating agents. This outstanding stability enabled quantitative functionalisation of the surface of BCN-23 with 24 available phosphonic acid groups.

The porosity of the new carboxylic or phosphonic acid-functionalised MOPs was assessed in CO_2-adsorption experiments at 200 K, which revealed that all the tested MOPs were porous to CO_2. Specifically, the maximum CO_2-uptake capacities at 1 bar were: 2.13 mmol/g (COOH–Bz-BCN-23); 1.61 mmol/g (COOH-C_5-BCN-23); 3.53 mmol/g (COOH-PEG_3-BCN-23); and 2.23 mmol/g (H_2PO_3-PEG_3-BCN-23) (Figure S64). Therefore, synthesised carboxylic or phosphonic acid-functionalised MOPs combine permanent porosity with on-surface coordination and covalent reactivity, making them ideal candidates as porous monomers in subsequent self-assembly processes.

Finally, we studied the pH-dependent solubility of all the synthesised carboxylic or phosphonic-acid functionalised MOPs. As expected, both types of MOPs were soluble in aqueous solution upon the stoichiometric deprotonation of the peripheral carboxylic or phosphonic acids, to obtain the corresponding carboxylate or phosphonate groups, respectively, affording negatively charged MOPs (Figure S36, S43, S50 and S58). However, the pH range in which each MOP was found to be water-soluble varied accordingly to its respective functionalisation (Figures S34, S41, S48 and S55). Thus, whereas carboxylic acid-functionalised MOPs precipitated out at pH 4.5 to 5.5, due to protonation of the surface COOH group, the phosphonic acid-functionalised one was soluble in water up to pH 2.7, which reflects the higher pK_a of carboxylic acids relative to phosphonic acid.

Synthesis and bio-recognition capabilities of biotinylated MOPs

Biotinylation of organic or inorganic nanoparticles, which involves attaching biotin molecules to their surface, has proven to be an effective method for enhancing their ability to interact with biological systems through the widely known biotin-streptavidin/avidin interaction.[30] For example, biotinylated nanoparticles have proven invaluable in the development of innovative biosensors and targeted delivery systems.[31,32] Consequently, as a first step towards the development of MOP-

based bioconjugates, we employed CuAAC for the biotinylation of MOPs, and then studied the resultant products for their interactions with avidin.

BCN-23 was biotinylated by reacting it with biotin-PEG_5-azide under the same standardised click conditions previously used for the model compounds. The structure of the product, hereafter named biotin-PEG_5-BCN-23, was confirmed by ^{1}H NMR in DMSO-d_6, which showed new broad signals that correspond to PEGylated biotin (Figure S59 and S60). DOSY NMR revealed the same diffusion coefficient ($D = 7.6 \cdot 10^{-11}$ m^2 s^{-1}) for these signals and for the aromatic peaks assigned to the MOP core (Figure S61). The calculated hydrodynamic radius was 2.5 nm in agreement with equilibrium configuration of the simulated structure (Figure 4a and S63). The incorporation of the PEG-biotin moiety onto the surface of BCN-23 was further confirmed by mass spectrometry, which revealed a broad peak that included the expected mass for $[Rh_{24}$(5-biotin-PEG_5-(−1H-1,2,3-triazol-4-yl)-bdc)$_{24} + H^+]^+$ of 19770 g/mol (Figure S62).

Next, we aimed to test the biorecognition capabilities of biotin-PEG_5-BCN-23. To this end, we employed the competitive HABA-avidin binding assay. In this assay, 2-(4-hydroxyphenylazo)benzoic acid (HABA) initially occupies the four possible binding sites of avidin (Figure 4b). When this interaction occurs, λ_{max} is centred at 500 nm, in contrast to the free form of HABA, whose λ_{max} is at 350 nm. The addition of free biotin to this complex induces the quantitative replacement of HABA due to the greater affinity of avidin for biotin ($K_d = 10^{-15}$) than for HABA ($K_d = 10^{-6}$). Therefore, the stoichiometric exchange between HABA and biotin can be followed through UV-Vis spectroscopy, by monitoring the changes in absorbance of the band centred at 500 nm (Figure S65). Thus, to study the biorecognition capabilities of MOP-bounded biotin moieties, we performed a competitive test in which increasing amounts of biotin-PEG_5-BCN-23 were added to separated aliquots of HABA-avidin at a constant concentration. The reaction mixture was maintained in solution up to the addition of one biotin-PEG_5-BCN-23 per avidin (i.e. 24 biotin molecules per avidin), after which partial precipitation was observed. The analysis of the aliquots that remained in solution revealed that biotin-PEG_5-BCN-23 does indeed recognise avidin. Furthermore, the molecular nature of the biotin-PEG_5-BCN-23 enabled calculation of the stoichiometry of these interactions. Thus, the average number of avidin groups attached to the MOP was found to be 1, irrespective of the excess amount of avidin in solution (Figure 4c and Figure S66-S68). This result implies that, once one avidin protein has attached to the MOP surface, there is strong steric hindrance that inhibits the recognition by the remaining 23 available biotin moieties on the surface. This steric hindrance might arise from the relative size of avidin (maximum cross section of ca. 8 nm) relative to the biotin-PEG_5-BCN-23 (diameter of ca. 5 nm), and/or to the mutual steric hindrance of surface-bound biotin groups, given their high surface density (*ca.* 0.5 biotin molecules per nm^2).

Conclusions

We have reported the synthesis of a novel alkyne-functionalised MOP that can be post-synthetically modified through CuAAC reactions. The CuAAC reaction proceeds quantitatively without compromising the structure of the parent MOP structure, which enables the synthesis of densely functionalised MOPs. We validated the scope of our approach by decorating the MOP surface with a wide range of chemically diverse substrates. For example, we synthesised novel MOPs with unprecedented functionalities, including carboxylic or phosphonic acid groups, or bioactive biotins. We envisage the use of CuAACs on "clickable" MOPs to further expand the repertoire of functional MOPs to guide the development of novel catalysts, sensors, and building blocks for hierarchical bio-mediated self-assembly processes.

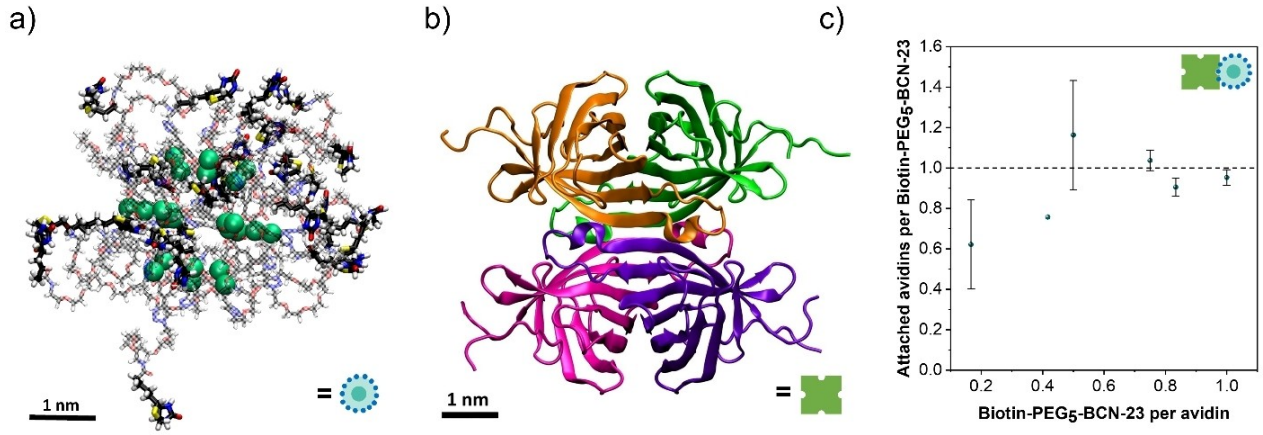

Figure 4. (a) Snapshot of the equilibrium structure of biotin-PEG_5-BCN-23 as obtained from molecular dynamics simulations in water solvent. Snapshots made with VMD.[17] Color code: Rhodium (green); carbon (black); hydrogen (white); oxygen (red); nitrogen (blue); Sulphur (yellow). Rh atoms are shown in their van der Waals size while linker is represented with Licorice drawing method. For simplicity, the MOP core is displayed as translucent. (b) Structure of avidin. (c) Plot of the average number of avidin proteins interacting with biotin-PEG_5-BCN-23 at different molar ratios of biotin-BCN-23/avidin.

Experimental Section

Synthesis of alkyne-protected Rh(II)-MOP: $Rh_2Ac_4 \cdot 2MeOH$ (20 mg, 0.04 mmol), H_2bdc-TIPS (74.4 mg 0.2 mmol) and Na_2CO_3 (25 mg, 0.2 mmol) were dispersed in 4 mL of DMA. The mixture was then transferred to a scintillation vial and heated at 100 °C for 48 h. A deep green solution was obtained and separated from the residual solids by centrifugation. The crude product was obtained by precipitation with water (20 mL) and then, separated by centrifugation. The solid was washed with water and dried by lyophilization. The resulting green solid was washed two times with methanol (20 mL) for further purification and dried in a vacuum oven at 85 °C overnight (93.9 mg, yield: 80 %).

Synthesis of BCN-23: The alkyne-protected Rh(II)-MOP (10 mg, 0.96 μmol) was dissolved in THF (1 mL). Then, tetrabutylammonium fluoride (34.7 μL, 34.7 μmol, 1 M solution in THF) was added to this solution under stirring, from which a blue precipitate appeared. This solid was rapidly centrifuged and subsequently washed three times with THF (2 mL) and dried under air.

General procedure to perform CuAAC reactions on BCN-23: BCN-23 (6.72 mg, 0.96 μmol) and the desired azide-functionalized ligand (34.56 μmol) were dissolved in DMSO (10 mL). Then, two aqueous solutions of sodium ascorbate (1.04 M) and $CuSO_4$ (0.7 M) were prepared. The addition of the required amount of catalyst (100 μL of $CuSO_4$ and 200 μL of sodium ascorbate) to complete the reaction was added stepwise in five additions over a period of 1.25 h under stirring. Once the additions were completed, the mixture was reacted at room temperature overnight. Finally, the obtained reaction products were separated and purified according to their solubility.

Synthesis of acid-functionalized Rh(II)-MOPs through CuAAC post-synthetic reactions: BCN-23 (6.72 mg, 0.96 μmol) and 34.56 μmol of 5-azidohexanoic acid (5.1 μL), 4-azidobenzoic acid (172.8 μL from a 0.2 M solution in tert-butyl ether) or COOH-PEG_3-N_3 (8.6 mg) were dissolved in DMSO (10 mL). The presence of free carboxylic acids in the reaction required the addition of acid to avoid precipitation during the reaction (20 μL, HCl 0.3 M). The CuAAC reaction were performed following the above-described general procedure. After the reaction, ethyl acetate (40 mL) was used to precipitate the product obtaining an orange coloured solid. These solids were washed once with a mixture of DMF: 0.3 M HCl (40 mL, 1 : 2) and twice with a DMF/H2O mixture (40 mL, 1 : 2). The final blue solids were dried in a vacuum oven at 85 °C for 2 h.

Synthesis of phosphonic acid-functionalized Rh(II)-MOPs through CuAAC post-synthetic reactions: BCN-23 (6.72 mg, 0.96 μmol) and H_2PO_3-PEG_3-N_3 (9.82 mg 34.56 μmol) were dissolved in DMSO (10 mL). Then, an aqueous solution (160 μL) containing THPTA (15.1 mg, 34.7 μmol) and $CuSO_4$ (10 μL from a 0.7 M solution, 6.94 μmol) was added to the mixture. Afterwards, sodium ascorbate (41.24 mg, 0.83 M) was added, and the mixture was reacted at room temperature overnight. Ethyl acetate (40 mL) was used to precipitate the product obtaining an orange-coloured solid that was subsequently washed once with 0.3 M HCl (40 mL) and twice with water (40 mL). Then, this purple coloured solid was dissolved in water (1 mL) using an aqueous solution of NaOH (46.24 μL, 1 M). The resulting purple solution was further purified using a dialysis procedure for 2 days. After that, a green solid was precipitated from the aqueous solution by treating it with a 3 M HCl until pH 1 was reached. Finally, the solid was lyophilized.

NMR adquisition. All 1D and 2D NMR experiments were acquired and processed under standard conditions. In particular, 2D DOSY experiments used a 150ms diffusion time and 2D ROESY experiments used a 400ms adiabatic mixing time. Other details can be found in the supporting information.

Acknowledgements

This work was supported by the Spanish MINECO (project RTI2018-095622-B–I00) and the Catalan AGAUR (project 2021 SGR 00458). It was also funded by the CERCA Programme /Generalitat de Catalunya and through a fellowship (LCF/BQ/PR20/11770011) from the "la Caixa" Foundation (ID 100010434). ICN2 is supported by the Severo Ochoa Centres of Excellence programme, Grant CEX2021-001214-S, funded by MCIN/AEI/10.13039.501100011033. A.C.S. is indebted to the Ramón y Cajal Program (RYC2020-029749-I Fellowship) and the Europa Excelencia grant (EUR2021-121997) L.H.L acknowledges the support from the Spanish State Research Agency (PRE2019-088056). C.v.B. thanks the Austrian Science Fund (FWF), Erwin Schrödinger fellowship for supporting the project J 4637. J. F acknowledges the financial support from MCIN/AEI/10.13039/501100011033 agency through Grant PID2021-124297NB-C33 and the "Severo Ochoa" Programme for Centres of Excellence in R\&D (CEX2019-000917-S) awarded to ICMAB. We also thank the Government of Catalonia (AGAUR) for Grant 2021SGR01519.

Conflict of Interests

The authors declare no conflict of interest.

Data Availability Statement

The data that support the findings of this study are available from the corresponding author upon reasonable request.

Keywords: biofunctionalization · click chemistry · metal–organic polyhedra · recognition · surface functionalisation

[1] M. Eddaoudi, J. Kim, J. B. Wachter, H. K. Chae, M. O'Keeffe, O. M. Yaghi, *J. Am. Chem. Soc.* **2001**, *123*, 4368–4369.
[2] A. Carné-Sánchez, J. Albalad, T. Grancha, I. Imaz, J. Juanhuix, P. Larpent, S. Furukawa, D. Maspoch, *J. Am. Chem. Soc.* **2019**, *141*, 4094–4102.
[3] T. Grancha, A. Carné-Sánchez, L. Hernández-López, J. Albalad, I. Imaz, J. Juanhuix, D. Maspoch, *J. Am. Chem. Soc.* **2019**, *141*, 18349–18355.
[4] J. Albalad, L. Hernández-López, A. Carné-Sánchez, D. Maspoch, *Chem. Commun.* **2022**, *58*, 2443–2454.
[5] G. A. Taggart, A. M. Antonio, G. R. Lorzing, G. P. A. Yap, E. D. Bloch, *ACS Appl. Mater. Interfaces* **2020**, *22*, 24913–24919.
[6] D. Zhao, S. Tan, D. Yuan, W. Lu, Y. H. Rezenom, H. Jiang, L.-Q. Wang, H.-C. Zhou, *Adv. Mater.* **2011**, *23*, 90–93.
[7] N. Hosono, M. Gochomori, R. Matsuda, H. Sato, S. Kitagawa, *J. Am. Chem. Soc.* **2016**, *138*, 6525–6531.
[8] G. Liu, Y. D. Yuan, J. Wang, Y. Cheng, S. B. Peh, Y. Wang, Y. Qian, J. Dong, D. Yuan, D. Zhao, *J. Am. Chem. Soc.* **2018**, *140*, 6231–6234.
[9] Y. Yang, T. K. Ronson, J. Zheng, N. Mihara, J. R. Nitschke, *Chem.* **2023**, *9*, 1–9.
[10] D. Luo, Z. J. Yuan, L. J. Ping, X. W. Zhu, J. Zheng, C. W. Zhou, X. C. Zhou, X. P. Zhou, D. Li, *Angew. Chem. Int. Ed.* **2023**, *62*, e202216977.
[11] V. J. Pastore, M. G. Sullivan, H. K. Welgama, M. R. Crawley, A. E. Friedman, C. Rumsey, M. Trebbin, J. Rzayev, T. R. Cook, *Chem. Mater.* **2023**, *35*, 1651–1658.
[12] J.-F. Lutz, Z. Zarafshani, *Adv. Drug Delivery Rev.* **2008**, *60*, 958–970.
[13] B. Gui, X. Liu, Y. Cheng, Y. Zhang, P. Chen, M. He, J. Sun, C. Wang, *Angew. Chem. Int. Ed.* **2022**, e202113852.
[14] M. Li, P. De, S. R. Gondi, B. S. Sumerlin, *Macromol. Rapid Commun.* **2008**, 1172–1176.

[15] P. M. E. Gramlich, S. Warncke, J. Gierlich, T. Carell, *Angew. Chem. Int. Ed.* **2008**, *47*, 3442–3444.
[16] P. M. E. Gramlich, C. T. Wirges, A. Manetto, T. Carell, *Angew. Chem. Int. Ed.* **2008**, 8350–8358.
[17] D. A. Roberts, B. S. Pilgrim, J. R. Nitschke, *Chem. Soc. Rev.* **2018**, *47*, 626–644.
[18] R. Chakrabarty, P. J. Stang, *J. Am. Chem. Soc.* **2012**, *134*, 14738–14741.
[19] T. Nakajo, S. Kusaka, H. Hiraoka, K. Nomura, N. Matsubara, R. Baba, Y. Yoshida, K. Nakamoto, M. Honma, H. Iguchi, T. Uchihashi, H. Abe, R. Matsuda, *Chem. Commun.* **2023**, *59*, 4974–4977.
[20] M. R. Dworzak, C. M. Montone, N. I. Haladzynski, G. P. A. Yap, M. O. Kloxin, E. D. Bloch, *Chem. Commun.* **2023**, *59*, 8977–8980.
[21] S. Furukawa, N. Horike, M. Kondo, Y. Hijikata, A. Carné-Sánchez, P. Larpent, N. Louvain, S. Diring, H. Sato, R. Matsuda, R. Kawano, S. Kitagawa, *Inorg. Chem.* **2016**, *55*, 10843–10846.
[22] J. Albalad, A. Carné-Sánchez, T. Grancha, L. Hernández-López, D. Maspoch, *Chem. Commun.* **2019**, *55*, 12785–12788.
[23] W. Humphrey, A. Dalke, K. Schulten, *J. Mol. Graphics* **1996**, *14*, 33–38.
[24] L. Hernández-López, J. Martínez-Esaín, A. Carné-Sánchez, T. Grancha, J. Faraudo, D. Maspoch, *Angew. Chem. Int. Ed.* **2021**, *60*, 11406–11413.
[25] Y. Lai, M. Li, M. Zhang, X. Li, J. Yuan, W. Wang, Q. Zhou, M. Huang, P. Yin, *Macromolecules* **2020**, *53*, 7178–7186.
[26] K. Omoto, N. Hosono, M. Gochomori, S. Kitagawa, *Chem. Commun.* **2018**, *54*, 7290–7293.
[27] M. Li, S. Jiang, J. Simon, D. Paßlick, M.-L. Frey, M. Wagner, V. Mailänder, D. Crespy, K. Landfester, *Nano Lett.* **2021**, *21*, 1591–1598.
[28] F. Steinke, L. Gemmrich Hernandéz, S. J. I. Shearan, M. Pohlmann, M. Taddei, U. Kolb, N. Stock, *Inorg. Chem.* **2023**, *62*, 35–42.
[29] S. Ondrušová, M. Kloda, J. Rohlíček, M. Taddei, J. K. Zaręba, J. Demel, *Inorg. Chem.* **2022**, *61*, 18990–18997.
[30] W. R. Algar, D. E. Prasuhn, M. H. Stewart, T. L. Jennings, J. B. Blanco-Canosa, P. E. Dawson, I. L. Medintz, *Bioconjugate Chem.* **2011**, *22*, 825–858.
[31] N. Nath, A. Chilkoti, *Anal. Chem.* **2002**, *74*, 504–509.
[32] K. Saha, S. S. Agasti, C. Kim, X. Li, V. M. Rotello, *Chem. Rev.* **2012**, *112*, 2739–2779.

Manuscript received: June 19, 2023
Accepted manuscript online: July 31, 2023
Version of record online: ■■, ■■

RESEARCH ARTICLE

Copper(I)-catalysed alkyne-azide cycloaddition click chemistry is a versatile post-synthetic tool to functionalize the surface chemistry of alkyne-functionalized cuboctahedral Metal–Organic Polyhedra (MOPs). This methodology enables quantitative functionalization of MOPs with a wide range of functional groups, including polymers, carboxylic and phosphonic acids and biomolecules.

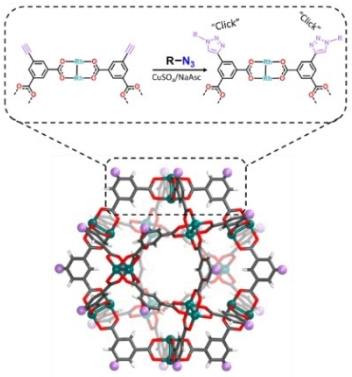

L. Hernández-López, Dr. C. von Baeckmann, Dr. J. Martínez-Esaín, A. Cortés-Martínez, Dr. J. Faraudo, C. Caules, Dr. T. Parella, Prof. Dr. D. Maspoch, Dr. A. Carné-Sánchez**

1 – 9

(Bio)Functionalisation of Metal–Organic Polyhedra by Using Click Chemistry